

Hemorrhages Detection in Fundus Image Based on Human Visual Characteristics

Jun Wu^{1,2} Dong-Xia Zhang^{1,2*} Song Yang^{1,2} Shu-Ya Song^{1,2}

¹Tianjin Polytechnic University, School of Electronics and Information Engineering, TianJin, China, 300387

²Tianjin Key Laboratory of Optoelectronic Detection Technology and System, TianJin, China, 300387

Corresponding author: Dong-Xia Zhang

Abstract: Hemorrhage is one of the early symptoms of diabetic retinopathy. Accurate detection of hemorrhages in fundus images is an important contribution for building automatic screening system of diabetic retinopathy, thus a novel algorithm based on human visual characteristics is proposed in this paper. Firstly, brightness correction and contrast limited adaptive histogram equalization are applied to fundus images. Secondly, candidate hemorrhages are extracted by background estimation and watershed segmentation. Thirdly, 2-D Gaussian fitting and human visual characteristics are used to extract visual characteristics of each candidate hemorrhage. Finally, hemorrhages are screened by support vector machine according to visual characteristics. The proposed method is evaluated on 219 fundus images of DIARETDB database. Experimental results show that overall average sensitivity, specificity and accuracy for hemorrhage in image level are 100%, 80% and 90.87% respectively, and overall average sensitivity and positive predictive value for hemorrhage in lesion level are 98.52% and 92.30% respectively. The results show that proposed method can realize automatic detection of hemorrhages in fundus image with high accuracy.

Keywords: fundus images; hemorrhage; watershed segmentation; human visual characteristics; support vector machine

Date of Submission 08-12-2017

Date of acceptance: 09-01-2018

I. INTRODUCTION

Diabetic Retinopathy (DR) is the most common and severe micro-vascular complication of diabetes mellitus. It is main cause of blinding in adults around the world. Fundus examination can not only timely detect DR, but also monitor other complications of diabetes. At present, there are various fundus examination methods at home and abroad. The method of fundus color photography is cheap, insensitive to drug and easy to record and save, thus it is considered as the most suitable method of DR screening by ophthalmologists. However the ophthalmologist check can't apply to large-scale DR screening, thus it is necessary to use computer technology to automatically identify the lesions in fundus image. Hemorrhages (HAs) are one of the early lesions of DR. Hemorrhages located in deep retina are usually dark red and round spots while hemorrhages located in shallow retina are usually bright red, linear, long strip or flamboyant spots. Hemorrhages usually coexist with micro-aneurysm, and the levels of DR in clinical are classified according to the presence or absence and the number of these two lesions. Therefore, accurate detection of HAs in color fundus images is of great significance for automatic screening and effective evaluation of DR.

In recent years, many scholars have studied automatic detection of HAs in fundus images, there are three main methods. The first method is template matching-based. For example, Bae et al.^[1] suggested a method using the normalized cross-correlation template matching. Gao et al.^[2] developed this research further and introduced multi-template matching. Xiao et al.^[3] proposed a method using adaptive templates matching. The second method is classifier-based. For example, Sirajudeen et al.^[4] used local binary pattern (LBP) and support vector machine (SVM) to classify targets for automatic detection of HAs. Caramihale et al.^[5] applied K-means clustering and artificial neural networks to detection of HAs. Santhakumar et al.^[6] used SVM to predict potential lesions and generated a classifier model to achieve detection of HAs. The third method is feature analysis-based. For example, Ashraf et al.^[7] used texture features to automatically detect HAs. Ganguly et al.^[8] used adaptive threshold method to achieve detection of red lesions. Pandey et al.^[9] used shape features to detect red lesions. In addition, there are some methods combined with several of the above methods. For example, Mane et al.^[10] detected red lesions by matching filtering and SVM classification. Hashim et al.^[11] detected HAs by haralick texture features, SVM and Multilayer Perceptron (MLP) classifiers. Although the above methods have realized automatic detection of HAs or red lesions, there are some problems such as high rate of false-positive and high rate of false-negative. Since HA usually does not have any fixed size or shape, template matching-based method is easy to be limited by size and shape of HA, so the robustness is poor. Classifier-based method is of high complexity and large computational complexity. Feature analysis-based

method is only based on one or several characteristics of HA, and does not fully consider essential characteristics of each structure in fundus image, so the applicability is not high.

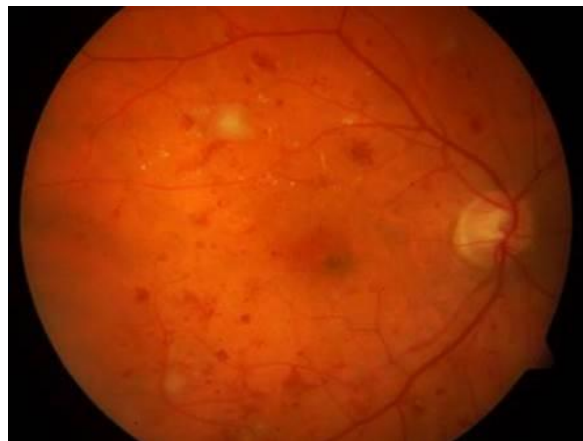
In summary, main reason for problems above is that characteristics of structures in fundus image are not adequately analyzed. Therefore, a method based on human visual characteristics is proposed in this paper. Firstly, brightness correction, green (*G*) channel extraction and contrast limited adaptive histogram equalization (CLAHE) are used to eliminate influence of uneven illumination and improve the contrast between HAs and background. Secondly, dark areas may be HAs are converted into bright areas by background estimation so that influence of background can be eliminated. Then, bright areas are divided into a plurality of candidate targets by watershed transformation, and HAs near blood vessel is separated from blood vessels to prevent missed detection of HA. Thirdly, candidate hemorrhages are estimated by 2-D Gaussian fitting for overcoming the limitations of traditional template matching, on the basis of which, characteristics of each structure such as HAs, vascular fragments, background texture mutation and noise in fundus image are analyzed and extracted by human visual characteristics. Finally, hemorrhages are screened from candidate hemorrhages by SVM according to visual characteristics.

II. PREPROCESSING

Original colored fundus image F_{or} may appear uneven brightness, low contrast phenomenon because of the influence of light and other factors, therefore, it is necessary to preprocess image F_{or} for improving its quality. The preprocessing mainly includes the following steps:

Step 1: To eliminate the uneven brightness, brightness correction is applied to the image F_{or} , that is, brightness value $V(i,j)$ is corrected to $B_c(i,j)$ according to eq. (1) in the HSV space. The result of brightness correction is shown in Fig. 1, where (a) is original color fundus image F_{or} , (b) is brightness corrected result image F_{bc} .

$$B_c(i, j) = \sqrt{1 - (V(i, j) - 1)^2} \quad (1)$$



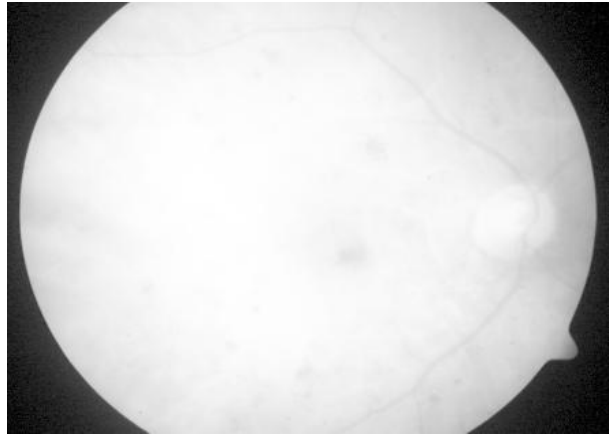
(a) Original Colored Fundus Image F_{or}



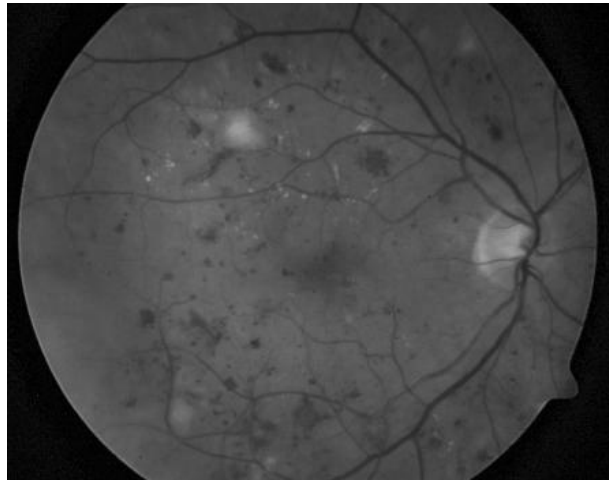
(b) Brightness Corrected Result Image F_{bc}

Fig. 1. Result of Brightness Correction

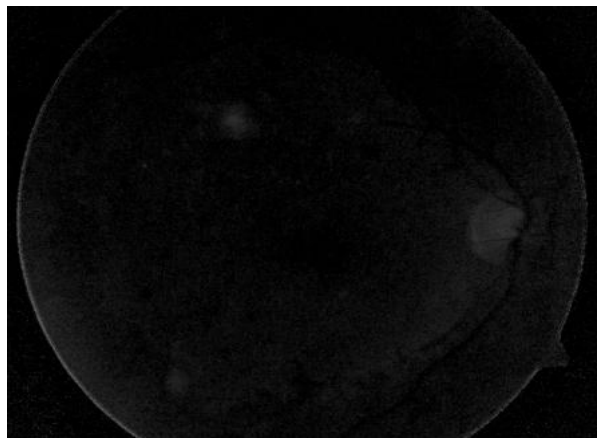
Step 2: Green channel of brightness corrected result image F_{bc} is extracted. Fig. 2 shows different components of image F_{bc} consist of red channel F_r , green channel F_g and blue channel F_b . It is clearly evident from the three channels of image F_{bc} that green channel contains the maximum information about hemorrhage. Therefore, green channel is used for further processing.



(a) Red Channel F_r



(b) Green Channel F_g



(c) Blue Channel F_b

Fig. 2. Each Channel of Image F_{bc}

Step 3: To improve the contrast between hemorrhages and background, Contrast Limited Adaptive Histogram Equalization (CLAHE) ^[12] is applied to green channel F_g . Fig. 3 shows the CLAHE processed image F_{pr} .

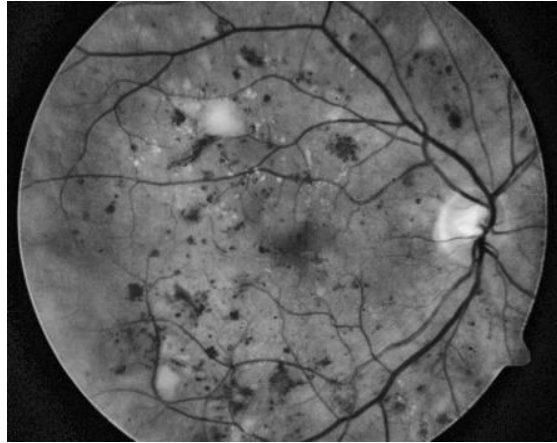


Fig. 3. CLAHE Processed Image F_{pr}

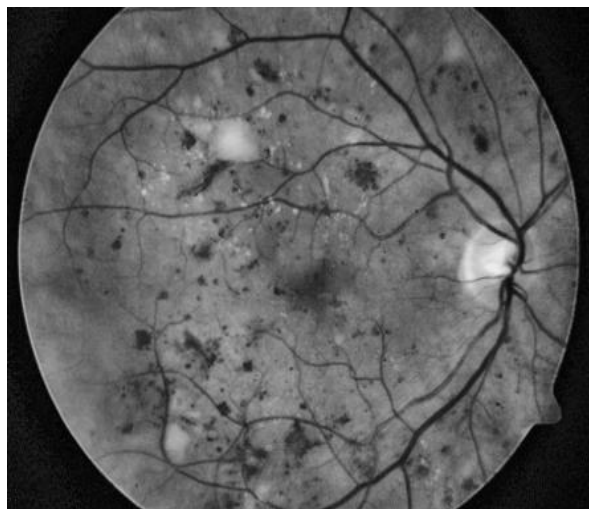
III. CANDIDATE HEMORRHAGES EXTRACTION

In addition to HAs, there are also blood vessels, background, background texture mutation and noise in F_{pr} , so it is necessary to extract regions of candidate hemorrhages. The traditional approach is threshold segmentation. However it is difficult to determine a fixed threshold for all images because of different quality of fundus image. In order to overcome above difficulties, this paper proposed a method based on background estimation and watershed segmentation to extract candidate targets. It mainly includes the following steps:

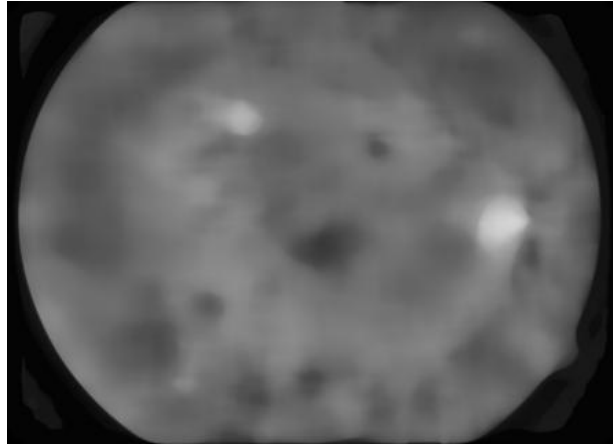
Step 1: Background estimation of the pre-processed image is performed to eliminate background effects. To ensure integrity of large hemorrhage, while not missing small hemorrhage, this paper firstly uses median filter with window size of 80×80 pixels to filter the image F_{pr} , obtaining approximate background image F_{mi} according to the size of fundus image and the proportion of hemorrhage in fundus image. Secondly, F_{pr} is subtracted from F_{mi} to obtain image F_{pm} . Thirdly, in order to reduce degree of over-segmentation caused by subsequent watershed segmentation, image F_{pm} is filtered three times with median filter of 3×3 pixels window, obtaining image F_{bm} . Finally, image F_{bm} is segmented with threshold value T that is variance of F_{bm} , obtaining image after background estimation.

$$F_{se}(i, j) = \begin{cases} F_{bm}(i, j), & F_{bm}(i, j) > T \\ 0, & \text{otherwise} \end{cases} \quad (2)$$

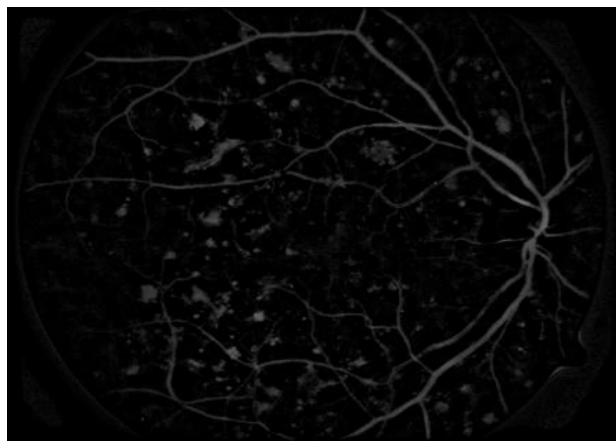
The process of background estimation is shown in Fig. 4, where (a) is the preprocessed image F_{pr} , (b) is the approximate background image F_{mi} , (c) is the difference image F_{pm} of F_{pr} and F_{mi} , (d) is the image F_{se} after background estimation. As seen from Fig. 4, preprocessed image F_{pr} contains a large number of backgrounds and background is not uniform. After background estimation, the dark area may be hemorrhages are transformed into bright area, which not only eliminates the influence of unevenness background, but also a large number of backgrounds are removed, thereby reducing number of candidate hemorrhages.



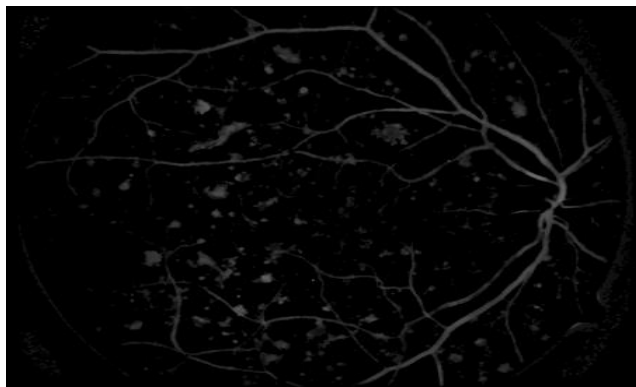
(a) Preprocessed Image F_{pr}



(c) Approximate Background Image F_{mi}



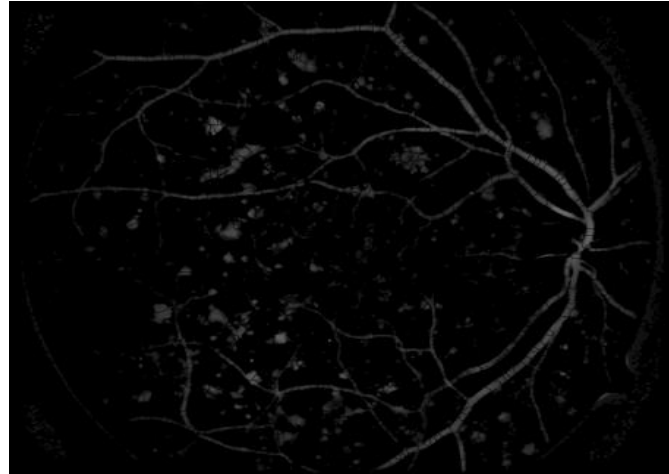
(c) Difference Image F_{pm} of F_{pr} and F_m



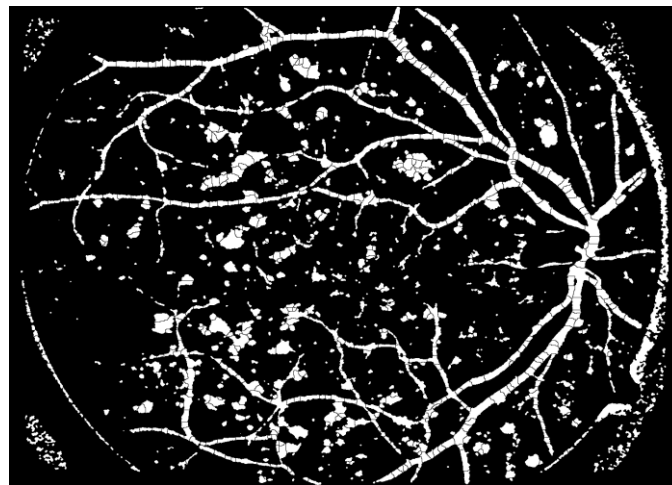
(d) Image F_{se} after Background Estimation

Fig. 4. Process of Background Estimation

Step 2: Image F_{se} is inverted and segmented by watershed transformation^[13], obtaining image F_{w_h} . Then image F_{w_h} is binarized with variance T as threshold to obtain result F_{w_b} of candidate hemorrhage extraction. Result of candidate hemorrhage extraction is shown in Fig. 5, where (a) is gray-scale image F_{w_h} after watershed segmentation, mainly includes the hemorrhages and some vascular fragments. Some hemorrhages are isolated while other hemorrhages are near blood vessels and easily detected as blood vessels in the detection of blood vessels. After watershed segmentation, hemorrhages near blood vessels are separated from blood vessels. (b) is binary image F_{w_b} after watershed segmentation, where hemorrhages with vascular adhesion have been divided into independent candidate targets, which helps to reduce missed detection rate of hemorrhages. Blood vessels are divided into vascular fragments, resulting in over-segmentation of blood vessels, which is important basis for subsequent detection of blood vessels.



(a) Gray-Scale Image F_{w_h} after Watershed Segmentation



(b) Binary Image F_{w_b} after Watershed Segmentation

Fig. 5. Result of Candidate Hemorrhages Extraction

IV. VISUAL FEATURES EXTRACTION

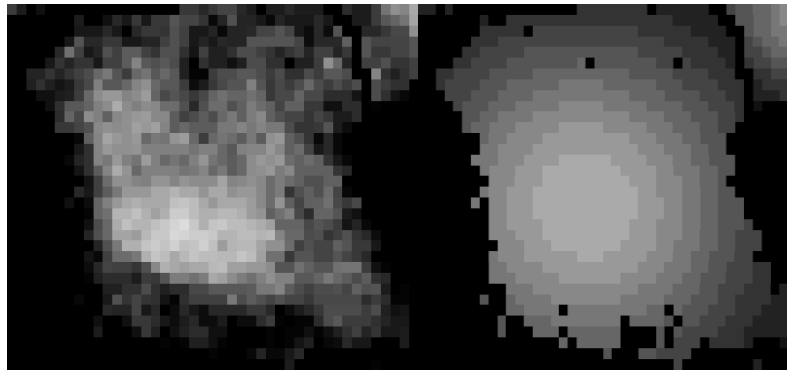
Gaussian fitting is usually used to estimate the Gaussian model parameters, then Gaussian fitting image is generated. Human visual characteristics are often used to evaluate the image quality intuitively. Therefore, this paper proposes a method based on 2-D Gaussian fitting and human visual characteristics to fit and extract visual characteristics for subsequent screening of HAs. It mainly includes two steps: 2-D Gaussian fitting and human eye visual features extraction.

Step 1: In order to improve the accuracy of fitting, this paper proposes a 2-D Gaussian model ^[14] with angle θ , which is expressed as follows:

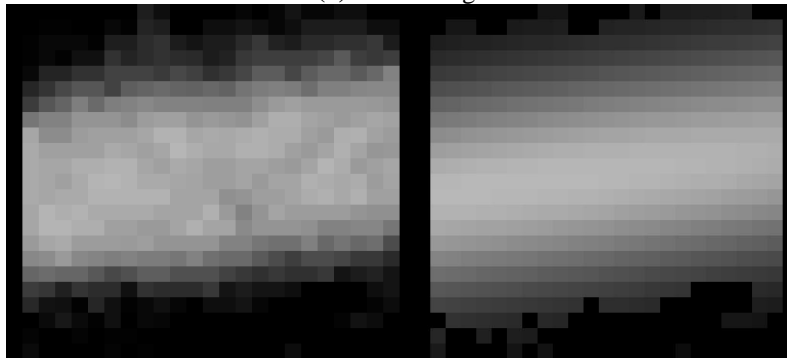
$$f(x, y) = A \times e^{-\left[\frac{x^2}{2\sigma_x^2} + \frac{y^2}{2\sigma_y^2}\right]} \quad (3)$$

$$\begin{cases} x' = (x - x_0) \cos \theta - (y - y_0) \sin \theta \\ y' = (x - x_0) \sin \theta + (y - y_0) \cos \theta \end{cases} \quad (4)$$

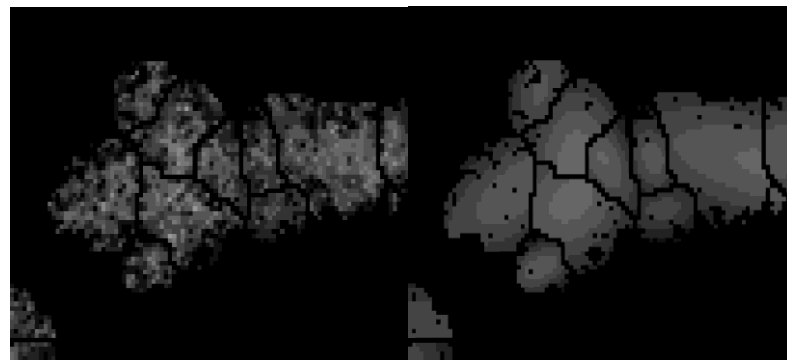
where (x_0, y_0) is the center coordinate of the Gaussian model, θ is the rotation angle, σ_x, σ_y are the standard deviations of x' and y' , respectively, and A is the Gaussian peak. Then four Gaussian model parameters above are used to fit candidate hemorrhage H_i . Candidate hemorrhages in F_{se} contain hemorrhage, vascular fragment, background mutation and noise, and their preprocessed result images and fitted result images are shown in Fig. 6.



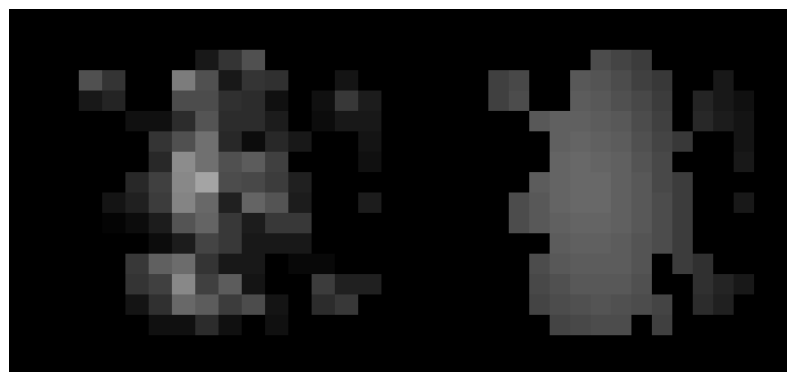
(a) Hemorrhage



(b) Vascular Fragment



(b) Background Texture Mutations



(d) Noise

Fig. 6. Result of Gaussian Fitting

Step 2: Based on 2-D Gaussian fitting, this paper proposes visual features (fitting error, ratio of space distance to its maximum value, texture change and proportional characteristic) of candidate hemorrhages are extracted by **Human Visual Characteristics**.

(1) Fitting error err

Fitting error refers to mean square value of difference image between candidate hemorrhage image H after pretreatment and candidate hemorrhage image G after fitting. The larger error err is, the higher noise content of candidate hemorrhage is, so fitting error err can be an index to judge noise. Fitting error of i -th candidate target is calculated as follows:

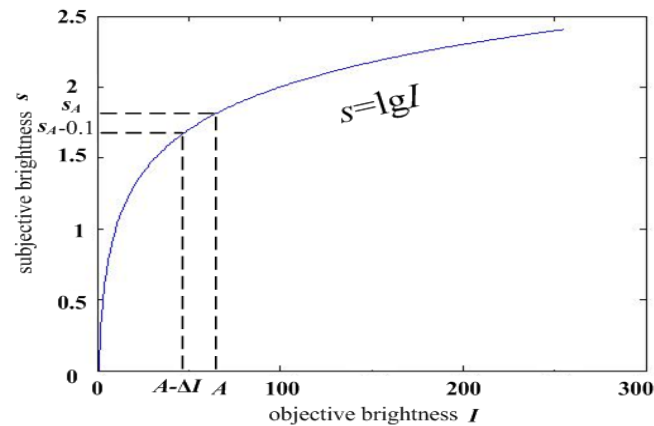
$$err(i) = \frac{\sum_{j=1}^{N_i} (H_i(x_j, y_j) - G_i(x_j, y_j))^2}{N_i} \quad (5)$$

(2) Ratio $\Delta d/l$ of spatial distance Δd to its maximum value l

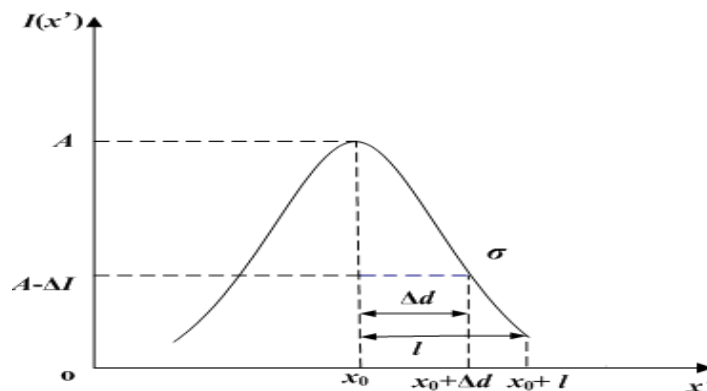
Subjective brightness is due to the fact that the light reflected by object illuminates retina of human eye and nerve is stimulated. Experiments show that there is a logarithmic relationship between subjective brightness and objective brightness, also known as Weber-Fechner's law [15].

$$s = k \lg I + k_0 \quad (6)$$

In this paper, the law is used to analyze degree of over-segmentation of candidate hemorrhages. The illustration is shown in Fig. 7, where (a) is curve of Weber-Fechner's law where $k=1, k_0=0$, ordinate represents subjective brightness s , and abscissa represents objective brightness, that is, gray level I . Assuming that x' axis is long axis of candidate target, curve of gray distribution is shown in (b), where the abscissa is the coordinate of spatial position x' , the ordinate is gray value $I(x')$ at corresponding position. The gray value at center point x_0 is A and its corresponding subjective brightness value is s_A . When subjective brightness s decreases from s_A to $s_A-0.1$, gray value decreases from A to $A-\Delta I$, and its corresponding spatial position changes from x_0 to $x_0+\Delta d$, and l is the maximum value of the spatial distance Δd . The greater ratio of Δd to its maximum l , the smaller gray-scale change in long axis observed by human eye, and the more severe degree of over-segmentation of HA, which only will occur in vascular fragments. Therefore, ratio $\Delta d/l$ is taken as an index for judging vascular fragments in this paper.



(a) Curve of Weber-Fickner's Law



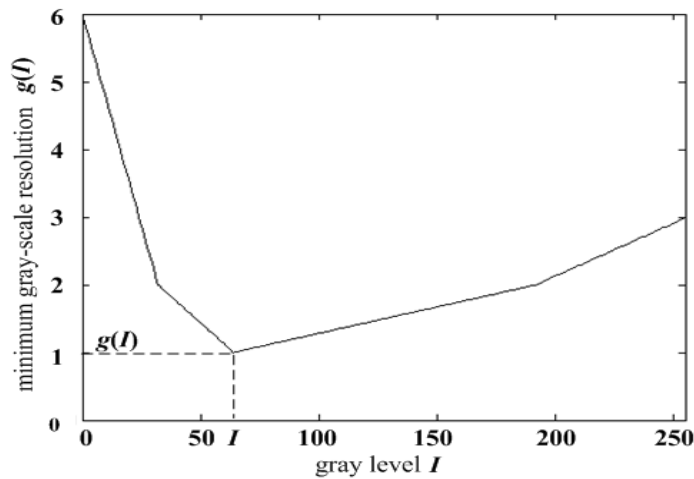
(b) Gray Distribution Curve of x' Axis

Fig. 7. Illustration of Degree of Over-Segmentation

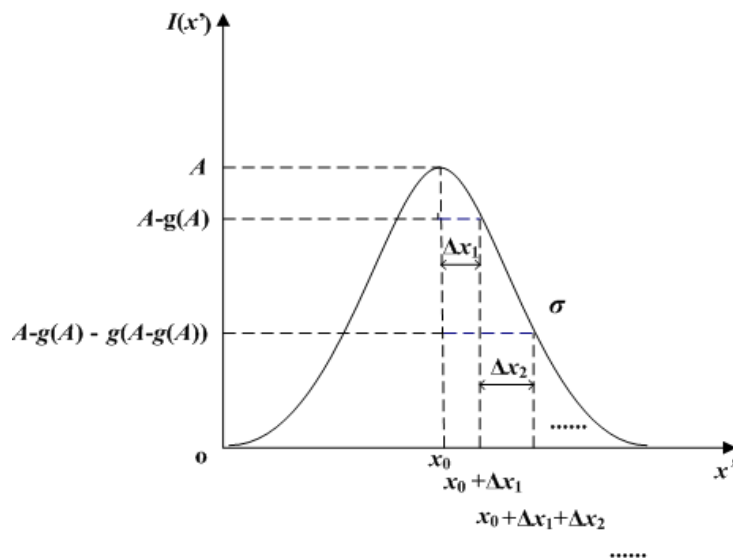
(3) Texture change $\Delta x_m, \Delta y_m$

Texture change is an important low-level visual feature. Sensitivity of human eye to change in gray-scale texture varies with the background brightness. For example, human eye is less sensitive to the detail of the image in high brightness background and low brightness background, but sensitivity of image detail in medium brightness background is higher. Experiments show that brightness difference human eye can only distinguish is function of I , that is, human eye gray-scale resolution characteristic^[16].

In this paper, human eye gray-scale resolution characteristic is used to analyze the texture change of the candidate target. Illustration of gray-scale texture change on the x' axis is shown in Fig. 8, where (a) is curve of the minimum gray-scale resolution $g(I)$ of human eye with the gray level I , (b) is curve of gray scale distribution on the x' axis of candidate hemorrhage, where abscissa is coordinate of spatial position x' , ordinate is gray value $I(x')$ at corresponding position. The gray value at center point x_0 is A and its corresponding distinguishable brightness difference is $g(A)$. When gray value decreases from A to $A-g(A)$, spatial position changes from x_0 to $x_0+\Delta x_1$, corresponding distinguishable brightness difference of gray value $A-g(A)$ is $g(A-g(A))$. When gray value decreases from $A-g(A)$ to $A-g(A)-g(A-g(A))$, spatial position changes from $x_0+\Delta x_1$ to $x_0+\Delta x_1+\Delta x_2$, and so on, a series of texture changes Δx_m ($m=1, 2, 3, \dots$) on the x' axis of candidate target can be obtained. Similarly, the minimum gray-scale resolution function is applied to y' axis, texture changes Δy_m ($m=1, 2, 3, \dots$) on y' axis of candidate target can be obtained. The smaller Δx_m and Δy_m is, the faster gray-scale texture changes is, the higher Gaussian significance is. Therefore, texture change $\Delta x_m, \Delta y_m$ is taken as an index for judging Gaussian significance.



(a) Curve of the Minimum Gray-Scale Resolution



(b) Gray Distribution Curve of x' Axis

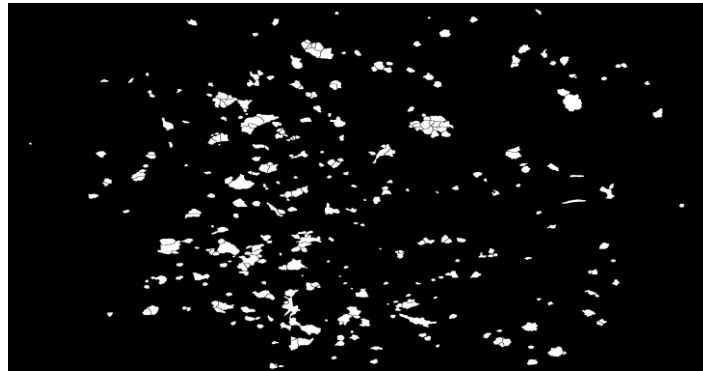
Fig. 8. Illustration of Texture Change

(4) Proportionality $\max(\Delta x_m, \Delta y_m) / \min(\Delta x_m, \Delta y_m)$

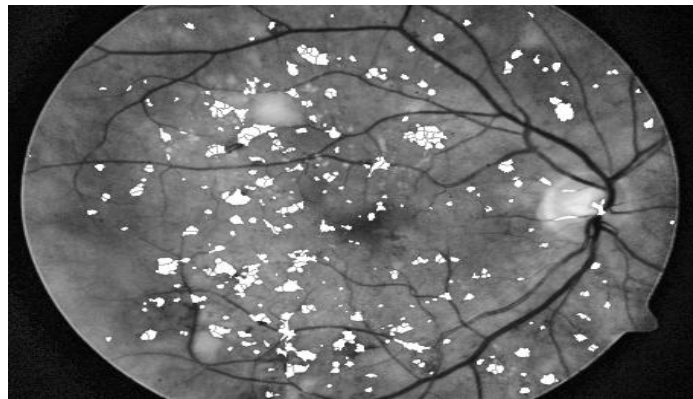
Proportionality refers ratio $\max(\Delta x_m, \Delta y_m) / \min(\Delta x_m, \Delta y_m)$ of texture change between long and short axis of candidate hemorrhage. $\max(\Delta x_m, \Delta y_m)$ is texture change on long axis of candidate target and $\min(\Delta x_m, \Delta y_m)$ is texture change on minor axis. The greater ratio $\max(\Delta x_m, \Delta y_m) / \min(\Delta x_m, \Delta y_m)$, the more obvious contrast of texture changes between long and short axis, the higher possibility of belonging to vascular fragment. Therefore, proportionality $\max(\Delta x_m, \Delta y_m) / \min(\Delta x_m, \Delta y_m)$ is taken as an index for judging vascular fragments.

V. SCREENING OF HA

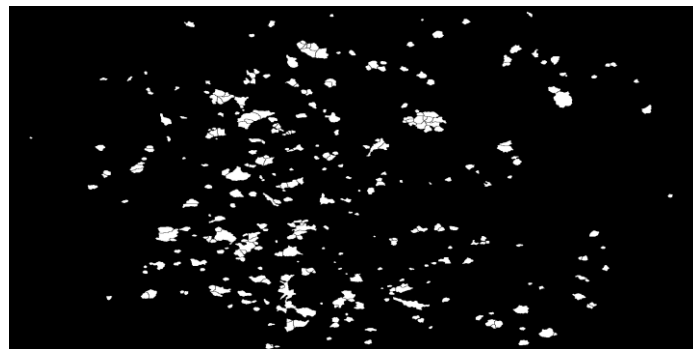
To get real hemorrhages, candidate hemorrhages need to be screened according to above visual characteristics including peak A , area N , texture changes on the minor axis Δx_m , the ratio $\Delta d/l$ of the spatial distance Δd to its maximum value l , proportionality $\max(\Delta x_m, \Delta y_m) / \min(\Delta x_m, \Delta y_m)$ and fitting error err . In this paper, SVM is used to screen HAs from candidate hemorrhages. 23 images in DIARETDB1 database are selected randomly as training set and other images are test set. Final detection result of hemorrhage is shown in Fig. 9, where (a) is result image of removing all false HAs, (b) is result image of removing all false HAs superimposed on F_{pr} , (c) is final detection result image of HAs, (d) is final detection result image of HAs superimposed on F_{pr} .



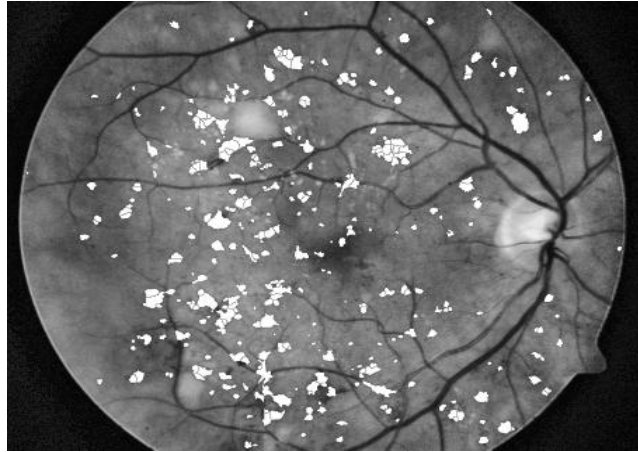
(a) Result Image of Removing All False Has



(b) Result Image of Removing All False HAs Superimposed on F_{pr}



(c) Final Detection Result Image of HAs



(d) Final Detection Result Image of HAs Superimposed on F_{pr}

Fig. 9. Final Detection Result

VI. EXPERIMENTAL RESULTS

Automatic hemorrhage detection method proposed in this paper was tested over a large database containing 219 colored fundus images of 1500×1152 , in which there are normal and varying lesion degrees images and corresponding ground-truth images manually marked by experts, thus it is of a certain representation. Parts of experimental results are shown in Fig. 10-12, where three original color fundus images (the 43th, 53th and 14th images of DB1 database) are shown in Fig. 10, and their detection results and ground-truth images are shown in Fig. 11 and Fig. 12, respectively. The lesion degree of three fundus images is increased according to international staging standards of DR.



(a) The 43th Image of DB1 Database



(b) The 53th Image of DB1 Database



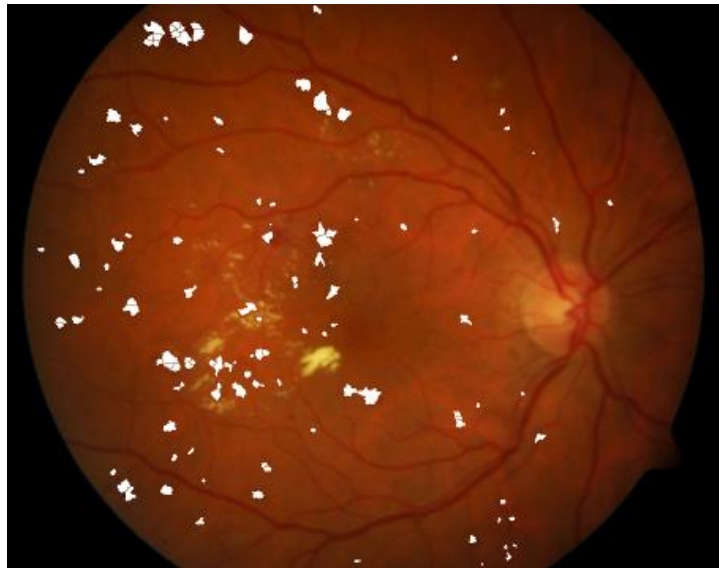
(c) The 14th Image of DB1 Database
Fig. 10. Varying Degrees of Lesion Images



(a) Detection Result of the 43th Image



(b) Detection Result of the 53th Image

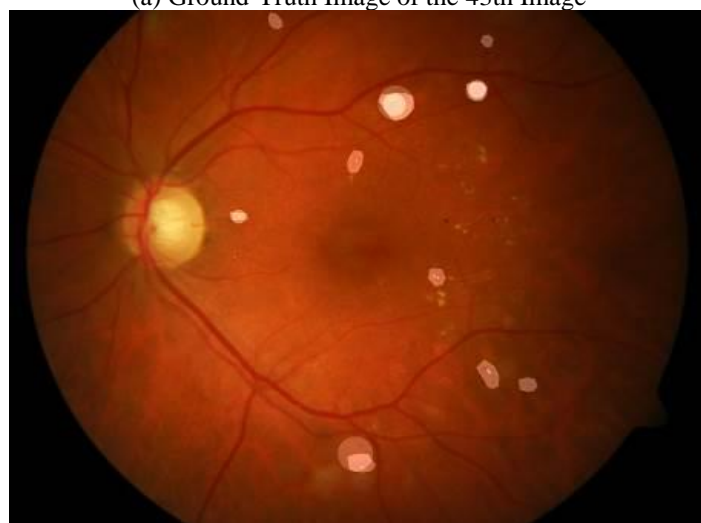


(c) Detection Result of the 14th Image

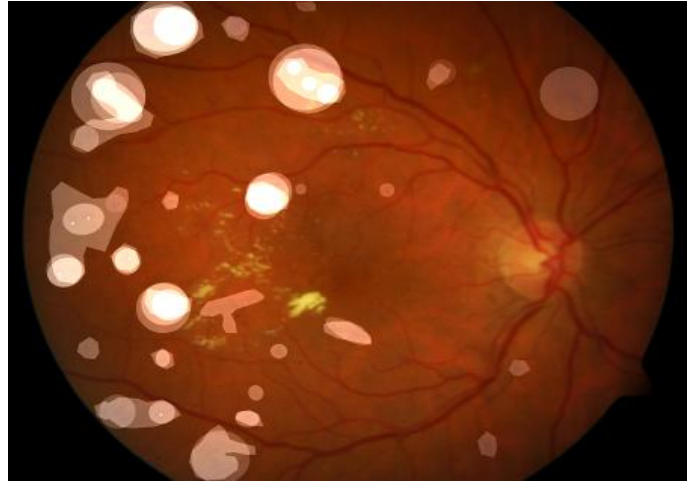
Fig. 11. Detection Results



(a) Ground-Truth Image of the 43th Image



(b) Ground-Truth Image of the 53th Image



(c) Ground-Truth Image of the 14th Image

Fig. 12. Ground-Truth Images

As revealed by Table. 1, evaluation of detection results is performed from image level and lesion level: overall average value of sensitivity (SE), specificity (SP) and accuracy (ACC) are used to evaluation of image level; Overall average of SE and positive predict value (PPV) are used to evaluation of lesion level. SE , SP , ACC , PPV are calculated as follows:

$$SE = \frac{TP}{TP + FN} \quad (7)$$

$$SP = \frac{TN}{TN + FP} \quad (8)$$

$$ACC = \frac{TP + TN}{TP + FN + TN + FP} \quad (9)$$

$$PPV = \frac{TP}{TP + FP} \quad (10)$$

where TP is true positive, FP is false positive, TN is true negative, FN is false negative. For the image (region) marked as hemorrhage by doctor, if it is consistent with detection result, then TP , otherwise FP ; For the image (region) marked as non-hemorrhage by doctor, if it is consistent with the detection result, then TN , otherwise FN .

The performance comparison between proposed method and other methods is shown in Table. 1, where literature [3] using adaptive template matching, literature [6] using machine learning, literature [8] using adaptive thresholds, are the representative methods of template matching, classifier and feature analysis, respectively. As seen from Table. 1, indicators of proposed method in image level and lesion level are mostly higher than other three methods, and missed detection rate of HAs is reduced to a large extent, improving sensitivity and accuracy of HA. The results show that proposed method has good detection performance.

Table. 1: Performance Comparison Between Proposed Method and Other Methods

Method	Image Level			Lesion Level	
	$SE/\%$	$SP/\%$	$ACC/\%$	$SE/\%$	$PPV/\%$
Method of Ref. [3]	100	80	92.40	89.01	87.30
Method of Ref. [6]	77	77	85	-	-
Method of Ref. [8]	87.71	94.62	-	-	-
Proposed Method	100	80	90.87	98.52	92.30

VII. CONCLUSION

Considering essential difference between HAs and other structures in fundus image, a detection method based on human visual characteristics is proposed. This method firstly uses watershed transformation to extract candidate hemorrhages, overcoming missed detection of HAs caused by threshold segmentation and detection of blood vessel. Then, Gaussian fitting of each candidate hemorrhage is carried out by using 2-D Gaussian model

with angle T , without considering HA's size, shape and other factors, overcoming limitations of template matching, then on the basis of which, intuitive visual characteristics of HAs, blood vessels, background texture mutation and noise in fundus image are extracted by human visual characteristics. Finally, hemorrhages are screened by SVM classifier according to visual features, access to the real HAs. Experiments show that proposed method can not only achieve accurate hemorrhage detection for different quality and different lesion degree of image, but also can effectively reduce missed detection rate of HAs.

REFERENCES

- [1]. Bae JP, Kim KG, Kang HC, et al. A study on hemorrhage detection using hybrid method in fundus images[J]. *Journal of Digital Imaging*, 2011, 24(3): 394.
- [2]. Gao WW, Shen JX, Wang YL, et al. Algorithm of locally adaptive region growing based on multi-template matching applied to automated detection of hemorrhages[J]. *Spectroscopy & Spectral Analysis*, 2013, 33(2): 448-453.
- [3]. Xiao ZT, Zhao BF, Zhang F, et al. Hemorrhages detection in fundus image based on k-means clustering and adaptive template matching[J]. *Chinese Journal of Biomedical Engineering*, 2015, 34(3): 264-71.
- [4]. Sirajudeen A, Ezhilarasi M. Multi-scale LBP and SVM classification to identify diabetic retinopathy in lesions[J]. *Current Medical Imaging Reviews*, 2015, 11(1): 527-38.
- [5]. Caramihale T, Dan P, Ichim L. Detection of regions of interest in retinal images using artificial neural networks and K-means clustering[C]// 22nd International Conference on Applied Electromagnetics and Communications. Dubrovnik: IEEE, 2016: 1-6.
- [6]. Santhakumar R, Tandur M, Rajkumar ER, et al. Machine learning algorithm for retinal image analysis[C]// IEEE Region 10 Conference. Singapore: IEEE, 2016: 1236-1240.
- [7]. Ashraf MN, Habib Z, Hussain M. Texture feature analysis of digital fundus images for early detection of diabetic retinopathy[C]// 11th International Conference on Computer Graphics, Imaging and Visualization (CGIV) - New Techniques and Trends. Singapore: IEEE, 2014: 57-62.
- [8]. Ganguly S, Ganguly S, Srivastava K, et al. An adaptive threshold based algorithm for detection of red lesions of diabetic retinopathy in a fundus image[C]// International Conference on Medical Imaging, M-Health and Emerging Communication Systems. Greater Noida: IEEE, 2015: 91-94.
- [9]. Pandey A, Chandra R, Dutta MK, et al. Automatic detection of red lesions in Diabetic Retinopathy using Shape based extraction technique in fundus image[C]// 39th International Conference on Telecommunications and Signal Processing. Vienna: IEEE, 2016: 538-542.
- [10]. Mane VM, Kawadiwale RB, Jadhav DV. Detection of red lesions in diabetic retinopathy affected fundus images[C]// IEEE International Advance Computing Conference. Bangalore: IEEE, 2015: 56-60.
- [11]. Hashim MF, Hashim SZM. Diabetic retinopathy lesion detection using region-based approach[C]// 8th Malaysian Software Engineering Conference. Langkawi: IEEE, 2014: 306-310.
- [12]. Reza A M. Realization of the contrast limited adaptive histogram equalization (CLAHE) for real-Time image enhancement[J]. *Journal of VLSI Signal Processing Systems for Signal Image & Video Technology*, 2004, 38(1): 35-44.
- [13]. Beucher S, Mathmatique CDM. The watershed transformation applied to image segmentation[J]. *Scanning Microscopy Supplement*, 1992, 6: 299-314.
- [14]. Feng XX, Zhang LY, Ye N, et al. Fast Algorithms on Center Location of Two Dimensional Gaussian Distribution Spot[J]. *Acta Optica Sinica*, 2012, 32(5): 0512002.
- [15]. Deco G, Scarano L, Sotofaraco S. Weber's law in decision making: integrating behavioral data in humans with a neurophysiological model[J]. *Journal of Neuroscience the Official Journal of the Society for Neuroscience*, 2007, 27(42): 11192.
- [16]. Avidan G, Harel M, Hendler T, et al. Contrast sensitivity in human visual areas and its relationship to object recognition[J]. *Journal of Neurophysiology*, 2002, 87(6): 3102.

Jun Wu . “Hemorrhages Detection in Fundus Image Based on Human Visual Characteristics.”
International Journal of Engineering Inventions, vol. 07, no. 01, 2018, pp. 51–65.